Millimeter Wave Channel Parameter Estimation Using a 3D Frequency Domain SAGE Algorithm

Rui Feng[1], Jie Huang[1], Jian Sun[1,2], Cheng-Xiang Wang[3,1], and Xiaohu Ge[4]
[1]Shandong Provincial Key Lab of Wireless Communication Technologies, Shandong University, Jinan, Shandong, 250100, China.
[2]State Key Lab. of Millimeter Waves, Southeast University, Nanjing, 210096, China.
[3]Institute of Sensors, Signals and Systems, School of Engineering & Physical Sciences, Heriot-Watt University, Edinburgh, EH14 4AS, U.K.
[4]School of Electronic Information and Communications, Huazhong University of Science and Technology, Wuhan, 430074, China.
Email: fengxiurui604@163.com, hj_1204@sina.cn, sunjian@sdu.edu.cn, cheng-xiang.wang@hw.ac.uk, xhge@mail.hust.edu.cn

***Abstract*—In order to describe the highly scattered property of millimeter wave (mmWave) multiple-input multiple-output (MIMO) channels, the existing high resolution frequency domain space-alternating generalized expectation-maximization (FD-SAGE) algorithm is studied and extended to three-dimentional (3D) MIMO case by including the estimation of elevation angles. The signal model and estimation procedure are described in detail and the capability of the proposed algorithm is verified in both synthetic and real measurement environments. Firstly, the performance of the proposed 3D FD-SAGE algorithm is evaluated in simulated single-input multiple-output (SIMO) channels. The estimation results match well with the parameter settings. Secondly, the impact of antenna array configuration and signal-to-noise ratio (SNR) on the capability of the proposed algorithm is also analyzed. It is found that systems with large antenna array size and high SNR exhibit excellent performance in angular estimation. Finally, 60 GHz mmWave indoor channel measurements are carried out and the channel parameters are estimated using the proposed 3D FD-SAGE algorithm.**

***Index Terms*—Parameter estimation, millimeter wave, 60 GHz, FD-SAGE.**

I. Introduction

Stimulated by the exploding requirements of wireless communications for human and devices connections, several key technologies such as massive MIMO, mmWave, visible light communication (VLC), and cognitive radio (CR) networks have been proposed to increase the data rate, network capacity, energy efficiency, and spectral efficiency [1]. The mmWave technology can provide large bandwidth to support Gigabits per second (Gbps) transmission data rate and the combination with massive MIMO and small cell networks can overcome high attenuation of mmWave [2], [3]. However, wireless communication systems using aforementioned technologies may exhibit different propagation characteristics, which bring new challenges to channel measurements and modeling. It is pointed out in [4] that, the massive MIMO and mmWave communication technologies will obviously reduce cell coverage, and in [5], mmWave MIMO communications with beamforming technique should take both azimuth and elevation angle characteristics into account. Thus, extensive channel measurements have been carried out in mmWave MIMO channels [6], [7], and high resolution parameter estimation methods including the estimation of elevation angles should be utilized to reveal the inherent phenomenon of the new channels.

There are mainly three categories of estimation methods to extract channel parameters from measurement data, i.e., spectral estimation, parametric subspace-based estimation, and deterministic parametric estimation. Multiple signal classification (MUSIC) and estimation of signal parameter via rotational invariance technique (ESPRIT) algorithms are representative for the first two categories, which perform far from satisfactory for highly correlated multipath components (MPCs) estimation. Within the third category are the expectation-maximization (EM) and SAGE algorithms. SAGE algorithm is an extension of EM algorithm by dividing the maximization procedure of all parameters into several subsets [8], and has been applied for joint estimation of amplitude, delay, azimuth angle of departure (AOD), elevation angle of departure (EOD), azimuth angle of arrival (AOA), elevation angle of arrival (EOA), and Doppler shift in time domain. For vector network analyzer (VNA) based channel measurements, it is more convenient to process the measurement data directly in frequency domain. FD-SAGE algorithm was proposed in [9] to estimate parameters including amplitude, delay, and AOA. In [10], estimation of AOD was involved to determine the angular characteristics at both ends of the radio link. However, the estimation of elevation angles at both ends is still absent in FD-SAGE algorithm.

Taking aforementioned problems into consideration, we introduce the frequency domain channel model, and extend the FD-SAGE algorithm to 3D case by taking elevation angles into account. Performance of the proposed algorithm is analyzed using synthetic data with different antenna array configurations and the value of SNRs. The VNA-based 60 GHz indoor channel measurements are also described and the channel parameters are estimated using the proposed 3D FD-SAGE algorithm.

The remainder of this paper is organized as follows. The time invariant MIMO channel model is outlined in Section II. Detailed introduction of 3D FD-SAGE algorithm is sketched in Section III. Performance and application of 3D FD-SAGE algorithm in synthetic data and real measurement data are presented in Section IV. Finally, conclusions are drawn in

Section V.

II. Signal Model

In a time invariant MIMO system consisting of M transmitter (Tx) antennas and N receiver (Rx) antennas, MPCs arrive at Rx with different delays, angles of departure, angles of arrival, and complex amplitudes. The double-directional channel impulse response (CIR) can be represented by summing L MPCs up [9],

$$h(\tau, \mathbf{\Omega}_T, \mathbf{\Omega}_R) = \sum_{l=1}^{L} \alpha_l \delta(\tau - \tau_l)\delta(\mathbf{\Omega}_T - \mathbf{\Omega}_{T,l})\delta(\mathbf{\Omega}_R - \mathbf{\Omega}_{R,l}) \tag{1}$$

where $\delta(\cdot)$ is the Dirac delta function, and notations α_l, τ_l, $\mathbf{\Omega}_{T,l}$, and $\mathbf{\Omega}_{R,l}$ are the complex amplitude, delay, AOD, and AOA of the l-th path, respectively. It is worth mentioning that $\mathbf{\Omega}_{(\cdot)}$ is a unit vector uniquely determined by azimuth and elevation angles, i.e., ϕ and θ. As depicted in Fig. 1, the initial point is anchored at a reference point and the terminal point is located on a sphere centering at the reference point with unit radius. Taking the impinging wave as an example, the direction of the arrival wave can be expressed in spherical coordinate,

$$\mathbf{\Omega}_R = e(\phi_R, \theta_R) = [\cos(\phi_R)\sin(\theta_R), \sin(\phi_R)\sin(\theta_R), \cos(\theta_R)]^{\mathrm{T}}, (\phi_R, \theta_R) \in [0, 2\pi) \times [0, \pi] \tag{2}$$

where $[\cdot]^{\mathrm{T}}$ denotes the transpose operator.

The channel transfer function can be obtained by Fourier transform (FT) of (1) in delay domain [10],

$$\mathbf{H}(f, \mathbf{\Omega}_T, \mathbf{\Omega}_R) = \sum_{l=1}^{L} \alpha_l \delta(\mathbf{\Omega}_T - \mathbf{\Omega}_{T,l})\delta(\mathbf{\Omega}_R - \mathbf{\Omega}_{R,l}) e^{-j2\pi f \tau_l} \tag{3}$$

where f represents the frequency. To obtain the frequency response matrix, the antenna radiation patterns are convolved to (3) as [11],

$$\mathbf{H}(f) = \sum_{l=1}^{L} \alpha_l \mathbf{c}_2(\mathbf{\Omega}_{R,l})\mathbf{c}_1^{\mathrm{T}}(\mathbf{\Omega}_{T,l}) e^{-j2\pi f \tau_l}. \tag{4}$$

At each frequency point, $\mathbf{H}(f)$ is a matrix of size $M \times N$. The frequency response of the measurement system is calibrated out before the measurements.

Steering vectors $\mathbf{c}_1(\mathbf{\Omega}_T)$ and $\mathbf{c}_2(\mathbf{\Omega}_R)$ represent the response of the arrays to a wave impinging from directions $\mathbf{\Omega}_T$ and $\mathbf{\Omega}_R$, which can be expressed as [12]

$$\mathbf{c}_1(\mathbf{\Omega}_T) = f_{T,m}(\mathbf{\Omega}_T)\exp\{j2\pi\lambda^{-1}\langle e(\mathbf{\Omega}_T), r_{T,m}\rangle\}, \quad m = 1, ..., M \tag{5}$$

$$\mathbf{c}_2(\mathbf{\Omega}_R) = f_{R,n}(\mathbf{\Omega}_R)\exp\{j2\pi\lambda^{-1}\langle e(\mathbf{\Omega}_R), r_{R,n}\rangle\}, n = 1, ..., N \tag{6}$$

where λ, $f(\mathbf{\Omega})$, and r denote the wavelength, complex antenna radiation pattern, and antenna location vector, respectively. The phase shift caused by antenna position is given as

$$\langle e(\mathbf{\Omega}), r\rangle = [x - d_x, y - d_y, z - d_z][\cos(\phi)\sin(\theta), \sin(\phi)\sin(\theta), \cos(\theta)]^{\mathrm{T}}. \tag{7}$$

As is shown in Fig. 1, x, y, and z are the position coordinates of the antenna element, and the spacing between adjacent antenna position in each axis is $d_x = d_y = d_z = \frac{\lambda}{2}$. Equation (7) shows the symmetry characteristics of the steering vector, which means horizontal planar array cannot distinguish impinging waves from above and below, and vertical planar array cannot distinguish impinging waves from front and back. Thus, cube, cylindrical and spherical antenna array, etc, would be better choices in order to acquire abundant angular information in channel measurements.

Further considering K frequency bins, the channel transfer function matrix at the k-th frequency bin is given as [10]

$$\mathbf{H}(k) = \sum_{l=1}^{L} \mathbf{S}(k; \boldsymbol{\theta}_l) + \mathbf{W}(k), 1 \le k \le K \tag{8}$$

where $\boldsymbol{\theta}_l = [\tau_l, \mathbf{\Omega}_{R,l}, \mathbf{\Omega}_{T,l}, \alpha_l]$ contains all the parameters of the l-th path, $\mathbf{S}(k; \boldsymbol{\theta}_l) = \alpha_l \mathbf{c}_2(\mathbf{\Omega}_{R,l})\mathbf{c}_1^{\mathrm{T}}(\mathbf{\Omega}_{T,l}) e^{-j2\pi f_k \tau_l}$ is the component contributed by the l-th path [8], and $\mathbf{W}(k)$ is the standard N-dimensional vector-valued zero-mean complex white Gaussian noise.

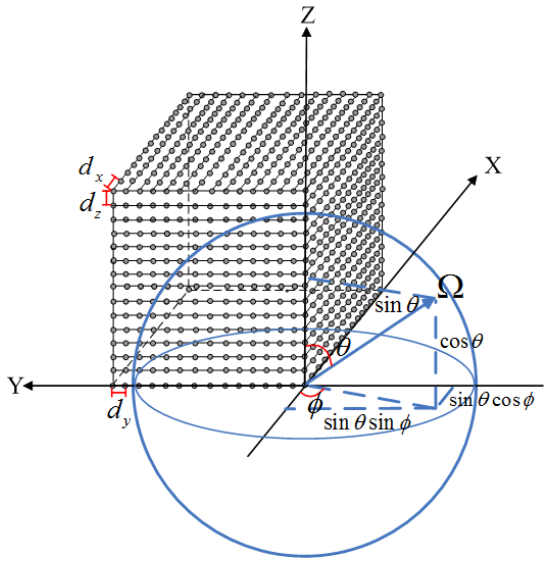

Fig. 1. Spherical coordinate and virtual cube antenna array configuration.

III. Parameter Estimation Using 3D FD-SAGE Algorithm

SAGE algorithm is an extension of EM algorithm by dividing the maximization procedure into several subsets. Complete data (unobservable) and incomplete data (observable) are two key notions of EM algorithm, and the choice of complete data should guarantee the rate of convergence for the parameter estimation procedure. As is shown in [13], the natural choice of complete data given in (9) leads to a simple scheme,

$$\mathbf{X}_l(k) = \mathbf{S}(k; \boldsymbol{\theta}_l) + \mathbf{W}(k), l = 1, ..., L. \tag{9}$$

The incomplete data is expressed as $\mathbf{H}(k) = \sum_{l=1}^{L} \mathbf{X}_l(k)$. If $\{\mathbf{X}_l(k), l = 1, ..., L\}$ is known, we can search the parameters of each path $\{\boldsymbol{\theta}_l, l = 1, ..., L\}$ that can maximize the maximum likelihood estimation (MLE) functions. As $\mathbf{X}_l(k)$ is unknown in practical, it can be obtained by subtracting all the paths except the l-th path from $\mathbf{H}(k)$,

$$\hat{\mathbf{X}}_l(k; \hat{\boldsymbol{\theta}}_{l'}^{'}) = \mathrm{E}[\mathbf{X}_l(k)|\mathbf{H}(k), \hat{\boldsymbol{\theta}}_{l'}^{'}] = \mathbf{H}(k) - \sum_{l'=1, l' \neq l}^{L} \mathbf{S}(k; \hat{\boldsymbol{\theta}}_{l'}^{'}). \tag{10}$$

Equation (10) represents the expectation (E) step of EM algorithm using parallel interference cancellation (PIC) method, where $\hat{\boldsymbol{\theta}}_{l'}^{'}$ denotes the initial assumption or previous estimation of the l'-th path.

Given the complete data acquired above, parameters of MPCs can be derived by searching for the values that can maximize the cost function [8],

$$\mathrm{z} = \mathbf{c}_2^{\mathrm{H}}(\boldsymbol{\Omega}_R) \sum_{k=1}^{K} e^{j2\pi f_k \tau} \hat{\mathbf{X}}_l(k; \hat{\boldsymbol{\theta}}_l^{'}) \mathbf{c}_1^{*}(\boldsymbol{\Omega}_T). \tag{11}$$

where $[\cdot]^{\mathrm{H}}$ and $[\cdot]^{*}$ denote Hermitian operator and complex conjugation. In the 3D FD-SAGE algorithm, parameters are divided into three sets: $\{\tau_l, \alpha_l\}$, $\{\boldsymbol{\Omega}_{T,l}, \alpha_l\}$, and $\{\boldsymbol{\Omega}_{R,l}, \alpha_l\}$, which are consecutively searched in each iteration step [10],

$$\hat{\tau}_l^{''} = \arg\max_{\tau} \{|\mathrm{z}(\tau, \hat{\boldsymbol{\Omega}}_{T,l}^{'}, \hat{\boldsymbol{\Omega}}_{R,l}^{'}; \hat{\mathbf{X}}_l(k; \hat{\boldsymbol{\theta}}_l^{'}))|\} \tag{12}$$

$$\hat{\boldsymbol{\Omega}}_{T,l}^{''} = [\hat{\phi}_{T,l}^{''}, \hat{\theta}_{T,l}^{''}] = \arg\max_{\boldsymbol{\Omega}_T} \{|\mathrm{z}(\hat{\tau}_l^{''}, \boldsymbol{\Omega}_T, \hat{\boldsymbol{\Omega}}_{R,l}^{'}; \hat{\mathbf{X}}_l(k; \hat{\boldsymbol{\theta}}_l^{'}))|\} \tag{13}$$

$$\hat{\boldsymbol{\Omega}}_{R,l}^{''} = [\hat{\phi}_{R,l}^{''}, \hat{\theta}_{R,l}^{''}] = \arg\max_{\boldsymbol{\Omega}_R} \{|\mathrm{z}(\hat{\tau}_l^{''}, \hat{\boldsymbol{\Omega}}_{T,l}^{''}, \boldsymbol{\Omega}_R; \hat{\mathbf{X}}_l(k; \hat{\boldsymbol{\theta}}_l^{'}))|\} \tag{14}$$

$$\hat{\alpha}_l^{''} = \frac{1}{MNK} \mathrm{z}(\hat{\tau}_l^{''}, \hat{\boldsymbol{\Omega}}_{T,l}^{''}, \hat{\boldsymbol{\Omega}}_{R,l}^{''}; \hat{\mathbf{X}}_l(k; \hat{\boldsymbol{\theta}}_l^{'})). \tag{15}$$

Equations (12)–(15) are referred to as the maximization (M) step. Iteratively carrying out the "E" and "M" steps, a sequence of estimates can be generated until the cost function converges to a stationary point.

Initialization of parameters for each path is also influential to the convergence rate of the iteration technique. Successive interference cancellation (SIC) method orders all the estimated waves in descending order according to the received power. It can avoid the inaccuracy estimation of weak MPCs caused by strong MPCs. With SIC method, "E" step in (10) can be rewritten as

$$\hat{\mathbf{X}}_l(k; \hat{\boldsymbol{\theta}}_l^{'}) = \mathbf{H}(k) - \sum_{l'=1}^{l-1} \mathbf{S}(k; \hat{\boldsymbol{\theta}}_{l'}^{'}). \tag{16}$$

Within the SIC initialization procedure, (12)–(14) can be replaced by (17)–(19) with pre-initial setting $\hat{\boldsymbol{\theta}}^{'} = [0, ..., 0]$ for each path. The initialization for all paths is consecutively carried out similar to the SAGE iteration procedure. Note that in the initialization procedure, we choose two-dimensional grid search scheme to estimate departure and incidence angles rather than one-dimensional search scheme, because the former would provide more accurate estimation of the direction information [13].

$$\hat{\tau}_l^{''} = \arg\max_{\tau} \{\sum_{m=1}^{M} \sum_{n=1}^{N} |\sum_{k=1}^{K} e^{j2\pi f_k \tau} \mathbf{X}_{l,m,n}(k; \hat{\boldsymbol{\theta}}_l^{''})|^2\} \tag{17}$$

$$\hat{\boldsymbol{\Omega}}_{T,l}^{''} = \arg\max_{\boldsymbol{\Omega}_T} \{\sum_{n=1}^{N} |\sum_{k=1}^{K} e^{j2\pi f_k \hat{\tau}_l^{''}} \mathbf{X}_{l,n}(k; \hat{\boldsymbol{\theta}}_l^{''}) \mathbf{c}_1^{*}(\boldsymbol{\Omega}_T)|^2\} \tag{18}$$

$$\hat{\boldsymbol{\Omega}}_{R,l}^{''} = \arg\max_{\boldsymbol{\Omega}_R} \{\sum_{m=1}^{M} |\mathbf{c}_2^{\mathrm{H}}(\boldsymbol{\Omega}_R) \sum_{k=1}^{K} e^{j2\pi f_k \hat{\tau}_l^{''}} \mathbf{X}_{l,m}(k; \hat{\boldsymbol{\theta}}_l^{''})|^2\}. \tag{19}$$

IV. Simulation Results and Analysis

A. Performance Evaluation in Simulated Environment

The 3D FD-SAGE algorithm analysis is performed over a bandwidth of 2 GHz centered at 60 GHz with 401 frequency sample points. A 1×64 SIMO channel with 20 MPCs is synthesized, and the MPC parameters are generated from distributions listed in Table I. Both AOA and EOA are taken into consideration as directional resolution is important especially in mmWave MIMO channel measurements. It is worth mentioning that the proposed algorithm is capable of double directional estimation, but only single directional channel data is simulated and measured in this paper as an example to illustrate the parameter estimation performance.

Fig. 2 shows a comparison of the estimated results with theoretical settings. The solid lines ended with stars and diamonds represent the theoretical settings and estimated parameters of 20 MPCs, respectively. The grid steps used to search delay and angles are 0.5 ns and 1°. It is clear to see that the simulation results of delay, AOA, and EOA for each path match very well with theoretical settings. From the results we can draw the conclusion that the proposed 3D FD-SAGE algorithm can provide accurate estimation in synthetic environment.

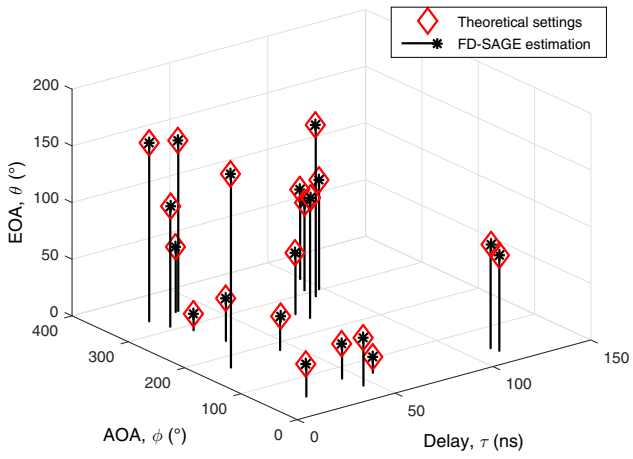

Fig. 2. Performance of 3D FD-SAGE algorithm in simulated environment.

It is verified in [9] that delays of MPCs can be estimated more precisely. We concentrate on observing the estimation results of AOA and EOA. While Fig. 2 is obtained under noise-less condition, in order to observe the estimation performance under different channel conditions, we choose $3 \times 3 \times 3$ cube array and simulate the channel with SNR equals to 5 dB and 20 dB, respectively. It is shown in Fig. 3(a) that several MPCs are not estimated accurately with SNR equals to 5 dB, while precise parameters can be extracted by increasing SNR to 20 dB.

Considering that antenna array configuration may has effects on the estimation results, we compare the estimated angles of arrival using virtual cube array and vertical planar array while keeping other parameters unchanged as listed in Table I. The planar array is a 8×8 vertical plane with total antenna number of 64. The results are shown in Fig. 3(b). It is clear that estimation results denoted in diamond, i.e., vertical planar array, cannot distinguish signals from front and back, while cube array denoted by circle match well with the simulation settings.

TABLE I
SIMULATION PARAMETER SETTINGS.

Parameter	Simulation setting
Number of Tx antenna, M	1
Rx array size, N	$4 \times 4 \times 4$ cube array
Carrier frequency, f	60 GHz
Bandwidth, B	2 GHz
Frequency bins, K	401
Number of paths, L	20
Amplitude, α	Complex zero-mean Gaussian distribution
Delay, $\tau(ns)$	Uniform distribution in [10, 130]
AOA, $\phi(^\circ)$	Uniform distribution in [0, 360]
EOA, $\theta(^\circ)$	Uniform distribution in [0, 180]

B. Application to Real Measurement Data

In this section, we apply the proposed algorithm to the real measurement data obtained in an indoor office environment. As is shown in Fig. 4, the room size is about $7.2 \times 7.2 \times 3$ m^3. It is furnished with multiple chairs, desks, several computers, and electronic devices. The walls, floor, and ceiling are made of concrete, and there are several windows on both sides of the wall.

The measurement system is consist of Keysight E8257D signal generator, Keysight N5227A VNA, 5-axes positioner, Tx and Rx antennas, and cables, etc. The measurement frequency range is from 59 GHz to 61 GHz and 401 frequency samples have been collected. Rx is a 10 dBi horn antenna located on the tripod with 1.6 m height, and Tx is an omni-directional antenna placed on positioner with the same height and scans in $15 \times 15 \times 15$ solid cube array. Tx and Rx antennas are aligned with distance of 4 m.

Channel parameters estimated via the 3D FD-SAGE algorithm are shown in Fig. 5. The power angular delay profile

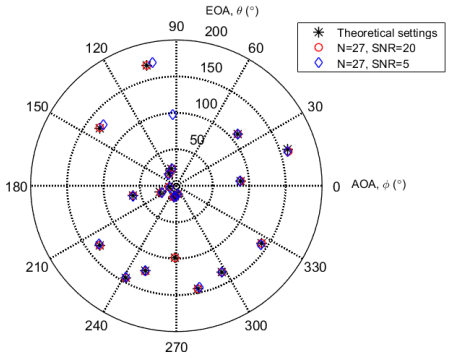

(a)

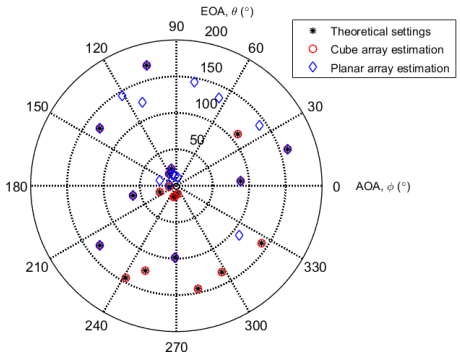

(b)

Fig. 3. Estimation results comparison under different array configurations and SNRs: (a) N=27, L=20, SNR=5 & 20 and (b) N=64, L=20, SNR=20.

Fig. 4. Real environment measurements.

(PADP) gives a clear illumination of the power, delay, AOD, and EOD of MPCs. Both the size and color of the circle are indicators of the received power. Totally 100 MPCs are estimated to represent all the dominant impinging waves. As Tx is aligned to Rx with 4 m distance, a strong line of sight (LOS) component with power gain up to -70 dB can be found with delay of 14 ns, which corresponds to the travel length with light speed. Waves arriving at Rx with delays around 28 ns are caused by first-order reflection.

Fig. 6 shows the estimated power angular profile (PAP). Azimuth angles of the estimated paths are centered at 0° and $\pm 180^\circ$, and the LOS component with azimuth angle of 0° and elevation angle of 90° agrees with the measurement environment setup. We can also see that the elevation angles of

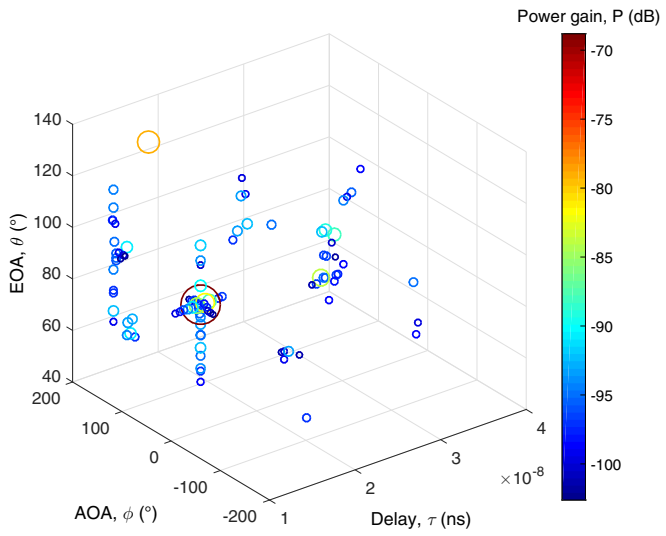

Fig. 5. Estimated delay-angular spread function.

estimated paths are dispersive, which verifies the significance of elevation angle estimation.

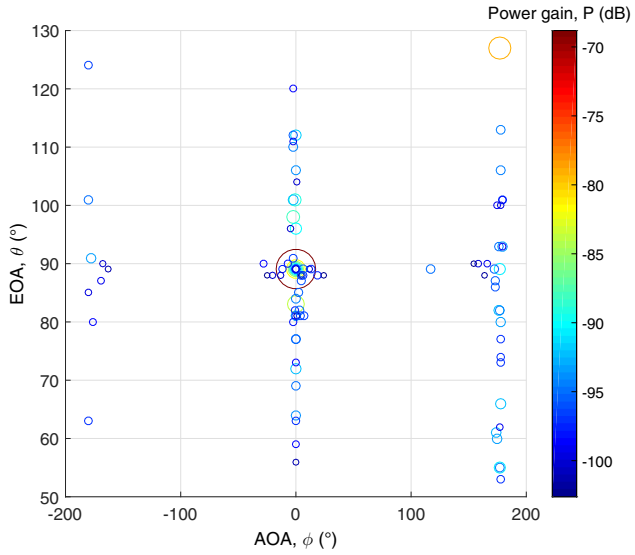

Fig. 6. Estimated power angular profile.

V. Conclusions

In this paper, a detailed derivation procedure of the frequency domain signal model with the features of steering vector has been introduced. Considering that elevation angles are of vital importance to describe mmWave MIMO channels, a 3D FD-SAGE algorithm has been proposed to jointly estimate the amplitude, delay, AOD, EOD, AOA, and EOA. In order to testify the performance of the proposed algorithm, a synthetic SIMO channel with 20 MPCs has been established. Results have shown that the estimated parameters match well with the settings. Simulations with different SNRs and array configurations have also been carried out. It has been shown that estimated results with high SNR and cube array perform better than that using low SNR and planar array. Channel measurements in a typical indoor office environment at 60 GHz have been described and analyzed using the proposed algorithm. The results have shown that the proposed 3D FD-SAGE algorithm can provide accurate parameter estimation and the dispersive elevation angles of MPCs further illustrates the importance of 3D angle estimation.

Acknowledgment

The authors would like to acknowledge the support from the EU H2020 ITN 5G Wireless project (Grant No. 641985), EU FP7 QUICK project (Grant No. PIRSES-GA-2013-612652), EPSRC TOUCAN project (Grant No. EP/L020009/1), 863 Project in 5G wireless networking (Grant No. 2014AA012101), and Natural Science Foundation of China (Grant No. 61210002).

References

[1] C.-X. Wang, F. Haider, X. Gao, X.-H. You, Y. Yang, D. Yuan, H. Aggoune, H. Haas, S. Fletcher, and E. Hepsaydir, "Cellular architecture and key technologies for 5G wireless communication networks," *IEEE Commun. Mag.*, vol. 52, no. 2, pp. 122–130, Feb. 2014.

[2] A. L. Swindlehurst, E. Ayanoglu, P. Heydari, and F. Capolino, "Millimeter-wave massive MIMO: the next wireless revolution?" *IEEE Commun. Mag.*, vol. 52, no. 9, pp. 56–62, Sept. 2014.

[3] X. Ge, S. Tu, T. Han, Q. Li, and G. Mao, "Energy efficiency of small cell backhaul networks based on Gauss-Markov mobile models," *IET Networks*, vol. 4, no. 2, pp. 158–167, Mar. 2015.

[4] X. Ge, H. Cheng, M. Guizani, and T. Han, "5G wireless backhaul networks: challenges and research advances," *IEEE Network*, vol. 28, no. 6, pp. 6–11, Nov. 2014.

[5] C. Gustafson, K. Haneda, S. Wyne, and F. Tufvesson, "On mmWave multipath clustering and channel modeling," *IEEE Trans. Antennas Propag.*, vol. 62, no. 3, pp. 1445–1455, Dec. 2013.

[6] X. Wu, Y. Zhang, C.-X. Wang, G. Goussetis, H. Aggoune, and M. M. Alwakeel, "28 GHz indoor channel measurements and modelling in laboratory environment using directional antennas," invited paper, in *Proc. EuCAP'15*, Lisbon, Spain, Apr. 2015.

[7] X. Wu, C.-X. Wang, J. Sun, J. Huang, R. Feng, Y. Yang, and X. Ge, "60GHz millimeter-wave indoor channel measurements and modeling for 5G systems," *IEEE Trans. Antennas Propag.*, accepted for publication.

[8] B. H. Fleury, M. Tschudin, R. Heddergott, D. Dahlhaus, and K. I. Pedersen, "Channel parameter estimation in mobile radio environments using the SAGE algorithm," *IEEE J. Sel. Areas Commun.*, vol. 17, no. 3, pp. 434–450, Mar. 1999.

[9] C. C. Chong, D. I. Laurenson, C. M. Tan, S. McLaughlin, M. A. Beach, and A. R. Nix, "Joint detection-estimation of directional channel parameters using the 2-D frequency domain SAGE algorithm with serial interference cancellation," in *Proc. IEEE ICC'02*, NewYork, USA, Apr. 2002, pp. 906–910.

[10] M. Matthaiou, D. I. Laurenson, N. Razavi-Ghods, and S. Salous, "Characterization of an indoor MIMO channel in frequency domain using the 3D-SAGE algorithm," in *Proc. IEEE ICC'07*, Glasgow, U.K., June 2007, pp. 5868–5872.

[11] T. Zwick, C. Fischer, and W. Wiesbeck, "A stochastic multipath channel model including path directions for indoor environments," *IEEE J. Sel. Areas Commun.*, vol. 20, no. 6, pp. 1178–1192, Aug. 2002.

[12] B. H. Fleury, P. Jourdan, and A. Stucki, "High-resolution channel parameter estimation for MIMO applications using the SAGE algorithm," in *Proc. IEEE IZSBC'02*, Zurich, Switzerland, Feb. 2002, pp. 30-1–30-9.

[13] B. H. Fleury, X. Yin, K. G. Rohbrandt, P. Jourdan, and A. Stucki, "Performance of a high-resolution scheme for joint estimation of delay and bidirection dispersion in the radio channel," in *Proc. IEEE VTC'02-Spring*, Birmingham, Alabama, May 2002, pp. 522–526.